APPLICATION OF COHERENT-OPTICAL METHODS IN PHYSICAL STUDIES OF EVAPORATION

S. B. Artemenko, A. T. Belonozhko, G. P. Vyatkin, Yu. G. Izmailov, S. A. Plokhov, and V. G. Rechkalov

UDC 536.423.16

The application of the methods of laser and holographic interferometry to the problems of measuring evaporation rates is examined. Mass transfer accompanying evaporation in the region of extradiffusion monitoring is studied.

The widespread use of evaporation processes in technological practice [1, 2] requires a detailed experimental study of mass transfer between the condensed and gas phases. The main characteristic in this case is the specific mass flow of vapor J_v, which must be measured accurately in order to determine the coefficients of condensation α_c (or coefficients of vaporization α_v) under conditions of evaporation into a vacuum [1, 3] or the coefficients of diffusion D under conditions of evaporation in a medium consisting of noncondensing gas [2]. It is also important to increase the measurement accuracy from the viewpoint of refining some theoretical assumptions, in particular, for clarifying the nature of the condensation coefficient, the experimental determination of which is the subject of a large number of works (see the review [4]). The wide range of values of α_c (over several orders of magnitude) is explained, in the opinion of Heiko and Cammenga in [5], not by physical factors, systematized in [3], but rather by methodical errors in the experiment.

The problem of measuring fluxes from the surface of the curved meniscus of a liquid is of independent interest. The presence of a curved interphase boundary, in most cases, in laboratory measurements of rates of evaporation from small open vessels can lead to errors when the results are transferred to the conditions of real technological apparatus. However, the use of average characteristics, such as the evaporation constant [6], for describing evaporation makes it much more difficult to compare the results obtained in experimental cells of different size.

The methods of holographic and laser interferometry enable not only increasing the accuracy of measurements of j_v but also studying the dependence of the flows on the cell geometry as well as the effect of temperature fields and the characteristics of heat and mass transfer at a three-phase boundary on the rate of evaporation.

The classical Michelson interferometer scheme, in which the surface of the liquid under study in the cell plays the role of the movable mirror, is not desirable, since the interference pattern characterizing the rate of evaporation is strongly perturbed owing to changes in the vapor concentration above the surface of evaporation. Because of this we proposed the interferometer shown in Fig. 1 for measuring evaporation rates. The interference pattern is formed by the beams reflected from the surface under study and the endface of the monofiber lightguide. To measure the difference in the rates of evaporation of liquids from cells of different size, one of the cells was placed in the measuring arm and the other in the reference arm of the Michelson interferometer. Laser interferometers enable measurements only for quite large evaporation surfaces. When the surface area decreases the curvature of the meniscus at the center of the cell increases. As a result a flat beam incident on the surface under study is curved when it is reflected from the surface. In narrow capillaries its curvature is so large that it is virtually impossible to perform measurements with the help of the laser interferometers studied.

The problem is solved, though with somewhat lower sensitivity, with the use of a holographic interferometer. The method consists essentially of first recording the hologram of

Chelyabinsk Interinstitute Service Center for Scientific Research. Translated from Inzhenerno-Fizicheskii Zhurnal, Vol. 55, No. 4, pp. 605-611, October, 1988. Original article submitted March 18, 1987.

 0022-0841/88/5504-1132$12.50

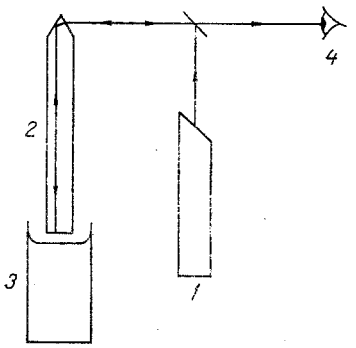

Fig. 1

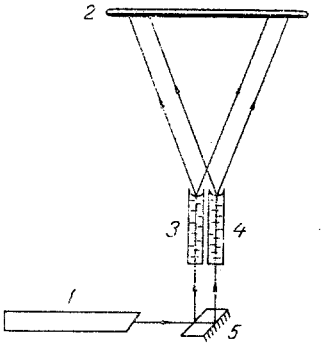

Fig. 2

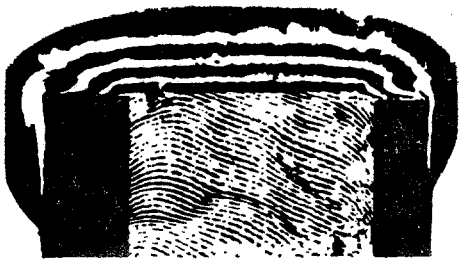

Fig. 3

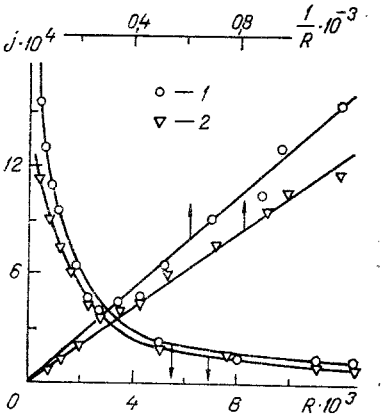

Fig. 4

Fig. 1. Interferometer for measuring the rate of evaporation: 1) laser; 2) monofiber lightguide; 3) cell with the liquid of interest; 4) direction of observation.

Fig. 2. Interferometer for measuring the relative rate of evaporation from cells with a small radius: 1) laser; 2) hologram; 3, 4) cells with the liquids of interest; 5) deflecting prism.

Fig. 3. Interferogram of the concentration of acetone vapor in the space above the cell.

Fig. 4. Dependence of the specific mass flux of vapor on the radius of the experimental cell (j is the specific mass flux of vapor, kg/(m²·sec); R is the radius of the cell, m): 1) ethyl alcohol; 2) isooctane.

the beam probing the liquid of interest in a quasiequilibrium state (the exposure time is quite short compared with the rates of the process under study) and the further study of the process is performed in real time.

The relative rate of evaporation from cylindrical vessels with a small radius was measured with the interferometer shown in Fig. 2. This variant of the interferometer gives the highest accuracy in measuring the rate of evaporation relative to some standard. We shall employ the specific mass flux $\langle j_V \rangle = (dm/d_\tau)/\pi R^2$, averaged over the cross-sectional area of the vessel, as the characteristic of the evaporation rate. It is shown in [7] that the meridional cross section of the resting drop for edge angles $\theta < \pi/2$ (which corresponds to a convex meniscus of the liquid in the cylindrical vessel) is approximated practically exactly by the equation of an ellipse. The meniscus in this case can be regarded as a spheroidal segment, whose volume is given by

$$V = \frac{1}{3}\pi R^2 h\left(\beta^2 + 1 - \beta\sqrt{\beta^2 - 1}\right) = \frac{1}{3}\pi R^2 h f(\beta), \tag{1}$$

where $\beta = b/R$.

The change in the height of the segment owing to evaporation $\Delta h = N\lambda/2$.

Thus, $\Delta m = \rho\Delta V = (1/6)\pi R^2 \rho N\lambda f(\beta)$ and we obtain for the flux

$$\langle j_v \rangle = \frac{1}{6}\rho\lambda f(\beta)\frac{dN}{d\tau}. \tag{2}$$

Therefore

$$\langle j_v \rangle = \langle j_v \rangle_{st} \frac{dN/d\tau}{(dN/d\tau)_{st}}.$$

The significant error associated with the fact that the semiaxes of the approximating spheroids do not coincide can be completely eliminated by working with flat meniscuses.

To determine the absolute values of the fluxes from the formula (2) an additional operation must be performed. This operation can be carried out in at least two ways.

1. The mass of the entire spheroidal segment can be determined (by separately weighing it or on a combined setup); knowing the mass, $f(\beta)$ can be calculated from the formula (1). The moment of evaporation of the entire segment as well as its height are recorded in the same interferometric experiment in which $dN/d\tau$ is measured.

2. The meridional profile of the miniscus can be calculated by solving numerically the problem of minimizing the potential energy functional of the meniscus [8, 9], and the parameters of the approximating spheroid can be found.

The method under study was employed to measure the rates of evaporation of distilled water, ethyl alcohol, benzene, acetone, and a number of other lqiuids. The gaseous medium was selected in all cases from the condition $\mu_{liq} > \mu_g$ in order to eliminate natural convection and ensure diffusive mass transfer. The satisfaction of these conditions is illustrated by the interferogram (Fig. 3) of the concentration fields of acetone vapor in air. For all liquids studied $\langle j_V \rangle$ increased as the radius of the vessel decreased (Fig. 4). The experimental data fall on a straight line in the $\langle j_V \rangle - 1/R$ plane.

The use of the spheroidal approximation enables obtaining analytical dependences $\langle j_V(R) \rangle$, adequately describing the experimental dependences, by analogy to the problem of the electric field of a conducting ellipsoid [10]. For quasistationary conditions the solution of Laplace's equation, written in ellipsoidal coordinates, with the boundary conditions $C(\lambda_e \to \infty) \to C_0$, $C(\lambda_e = 0) = C_p$ has the form

$$C(\lambda_e) = C_0 + \frac{C_p - C_0}{\operatorname{arctg}\sqrt{\frac{b^2}{a^2} - 1}} \operatorname{arctg}\sqrt{\frac{b^2 - a^2}{\lambda_e + a^2}}.$$

The specific mass flux in the vicinity of this point $j_V(\lambda_e = 0) = -D(\partial C/\partial n|_{\lambda=0})$, taking into account the relation between the ellipsoidal and Cartesian coordinates, is determined by the expression

$$j_v(r) = \frac{D(C_p - C_0)\sqrt{b^2 - a^2}}{\sqrt{b^4 - r^2(b^2 - a^2)}\operatorname{arctg}\sqrt{b^2/a^2 - 1}}.$$

Averaging according to the formula $\langle j_v \rangle = \frac{1}{\pi R^2}\int_S j_v(r)\,dS$, we obtain

$$\langle j_v \rangle = \frac{2D(C_p - C_0)}{R} \frac{f(\alpha, \beta)}{\alpha \operatorname{arctg} f(\alpha, \beta)}, \tag{3}$$

where $f(\alpha, \beta) = \sqrt{\alpha^2(\beta - \sqrt{\beta^2 - 1}) - 1}$; $\alpha = R/h$; $\beta = b/R$.

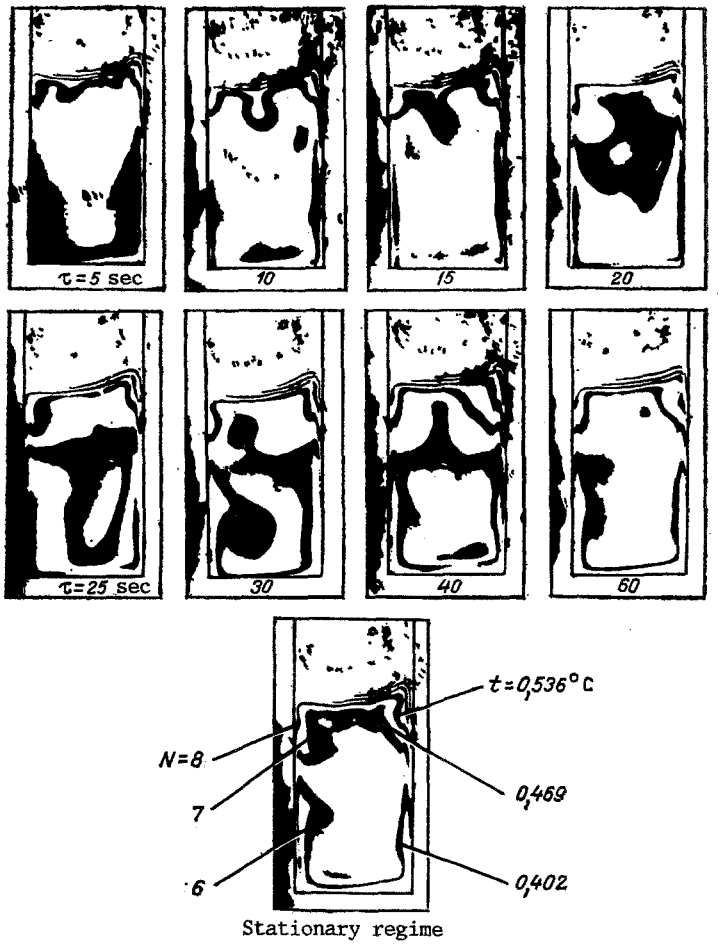

Fig. 5. Motion picture of the change in the temperature field of a liquid in the process of evaporation. t is the temperature of the liquid in °C and τ is the time from the start of the experiment in sec.

As follows from (3), $\langle j_V \rangle$ is inversely proportional to the radius of the vessel; this agrees with the experimental data. In addition to qualitative agreement, there is also quantitative agreement. The coefficients of diffusion calculated from (3) for the systems shown in Fig. 4 equal $D_{H_2O} = 2.51 \cdot 10^{-5}$ m²/sec, $D_{C_2H_5} = 4.96 \cdot 10^{-5}$ m²/sec, $D_{C_6H_6} = 9.23 \cdot 10^{-5}$ m²/sec. The maximum deviation from the tabulated values [11] is observed for benzene and equals 6.1%.

The reliability of the results obtained depends strongly on the existence of temperature gradients along the surface of evaporation; such gradients could be present owing to different conditions of heat transfer at the center and at the periphery. The sections of the meniscus surface near the three-phase boundary, unlike surface sections, are located in the zone of two heat fluxes: from the walls of the vessel and from the bulk of the liquid. This difference will exist under conditions when the temperature of the surrounding medium is maintained constant; this leads to more intense heat transfer at the periphery and can affect the distribution of the specific mass fluxes $j_V(r)$ over the cross section of the meniscus.

To study these questions the temperature fields of the liquids mentioned were investigated with the help of a holographic interferometer [12]. The temperature field in the liquid was recorded as follows. The cell with the liquid was covered tightly with a top and held until the equilibrium state was established; the moment at which this state appeared was established from the termination of the motion of the interference pattern in the interferometer, in which a diffraction grating, obtained based on the same scheme, but without object, was placed at the location of the hologram. After the hologram was recorded the top on the cell was opened and the state of equilibrium was destroyed; this changed the temperature field of the liquid in the process of evaporation. The fringes passing through the center of the cell were counted with the help of a reversible counter. The direction of increasing fringe order was determined with a compensator.

The interference pattern was interpreted with the help of the values of dn/dT, determined by Shedel [13]. It is known from [14] that the character of the dependence of the refractive index n on T for organic liquids is described by a smooth curve in the temperature range from 20 to 40°C, while at temperatures from 20 to 30°C dn/dT changes by less than 1%. For this reason, because of the smallness of the change in the temperature in the experiment (of the order of 1 K) dn/dT can be regarded as constant. The temperature was calculated with the help of the following dependence: $T = T_p + \Delta n/(dn/dT)$, $\Delta n = N\lambda/\ell$.

Figure 5 shows examples of interferograms of temperature fields of liquids in the process of evaporation.

The calculations showed that in all cases the radial temperature gradient on the surface of the meniscus differs from zero and is directed from the center to the periphery. However, in no case does the temperature difference $T_{r=0} - T_{r=R}$ at the temperatures of the experiment (295-297 K) exceed 1 K. Thus, for acetone $\Delta T = 0.06$ K and for alcohol $\Delta T = 0.08$ K. The difference of the temperatures between the volume and the surface of the liquid is also small and equals 0.25 K for the central zone of the meniscus. Thus, $\Delta T \ll T$, and at these temperatures the method described above can be employed to calculate the fluxes and coefficients of diffusion without taking into account the nonisothermal nature of the meniscus.

NOTATION

j_v is the specific mass flux of the vapor, kg/(m²·sec); α_c, coefficient of condensation; α_v, coefficient of evaporation; D, coefficient of diffusion, m²/sec; θ, wetting angle; R, radius of the vessel, m; τ, time, sec; h, height of the segment, m; λ, wavelength of the laser radiation, m; N, order of the interference fringe or the number of fringes passing through a given point; ρ, density of the matter, kg/m³; ℓ, length of the cell with the liquid of interest, m; T, temperature, K; n, refractive index of the medium; m, mass, kg; V, volume of the spheroidal segment, m³; μ_{liq} and μ_g, molar mass, kg/mole; C_0 and C_p, concentration of vapor in the gas, kg/m³; a and b, semiaxes of the spheroid, m; λ_e, ellipsoidal coordinate of a point on the surface, m²; $\partial c/\partial n$, derivative along the normal; r, coordinate of a point on the surface of evaporation, m; $\pi = 3.141$; Δn, change in the refractive index of the medium. The indices denote the following: st, standard liquid; liq, liquid; g, gas; 0, starting state; p, equilibrium pressure.

LITERATURE CITED

1. M. I. Ivanovskii, V. P. Sorokin, and V. I. Subbotin, Evaporation and Condensation of Metals [in Russian], Moscow (1976).
2. R. Hiecke and M. Schubert, Verdunstungsvorgange – Theorie und technische Anwendung, Leipzig (1976).
3. D. Hirs and G. Pound, Evaporation and Condensation [Russian translation], Moscow (1966).
4. N. I. Kochurova, Problems in the Thermodynamics of Heterogeneous Systems and the Theory of Surface Phenomena [in Russian], No. 3, Leningrad (1975), pp. 154-170.
5. H. K. Cammenga, Curr. Top. Sci., 5, 335-446 (1980).
6. B. M. Lepinskikh and A. I. Manakov, Physical Chemistry of Oxide and Oxyfluoride Melts [in Russian], Moscow (1977).
7. W. M. Robertson and G. W. Lehman, J. Appl. Phys., 39, No. 4, 1994-2002 (1968).
8. M. A. Belyaeva, L. A. Slobozhanin, and A. D. Tyuptsov, Introduction to the Dynamics of a Body with a Liquid Under Zero-g Conditions [in Russian], Moscow (1968), pp. 5-68.
9. F. L. Chernous'ko, ibid., pp. 69-97.
10. L. D. Landau and E. M. Lifshits, Theoretical Physics, Vol. 8, Electrodynamics of Continuous Media [in Russian], Moscow (1982).
11. I. B. Vargaftik, Handbook of the Thermophysical Properties of Gases and Liquids [in Russian], Moscow (1972).
12. A. K. Beketova et al., Holographic Interferometry of Phase Objects [in Russian], Leningrad (1979).
13. C. West, Holographic Interferometry [Russian translation], Moscow (1982).
14. V. P. Frantas'ev and A. S. Shraiber, Zh. Fiz. Khim., 43, 425-429 (1969).